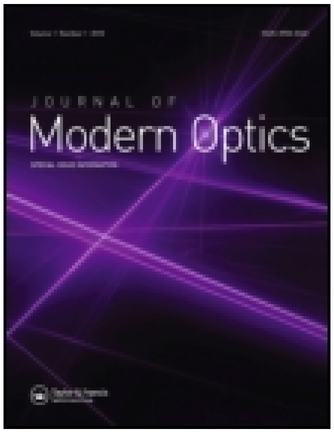

Journal of Modern Optics
Publication details, including instructions for authors and subscription information:
http://www.tandfonline.com/loi/tmop20

Novel narrow-band spectral interference filter with very high transmittance

J. Bogdanski [a], A. Danan [b], S. Jobling [a], K.T. McCusker [a], S. Quint [c], A.Z. Smith [a], J. Smith [a] & P.G. Kwiat [a]

[a] Department of Physics, University of Illinois at Urbana-Champaign, Urbana, Illinois, USA

[b] School of Physics and Astronomy, Raymond and Beverly Sackler Faculty of Exact Sciences, Tel-Aviv University, Israel

[c] Johannes Gutenberg University, Mainz, Germany

Published online: 07 Jan 2011.

Journal of Modern Optics
Vol. 58, Nos. 3–4, 10–20 February 2011, 306–311

Novel narrow-band spectral interference filter with very high transmittance

J. Bogdanski[a]*, A. Danan[b], S. Jobling[a], K.T. McCusker[a], S. Quint[c], A.Z. Smith[a], J. Smith[a] and P.G. Kwiat[a]

[a]*Department of Physics, University of Illinois at Urbana-Champaign, Urbana, Illinois, USA;* [b]*School of Physics and Astronomy, Raymond and Beverly Sackler Faculty of Exact Sciences, Tel-Aviv University, Israel;* [c]*Johannes Gutenberg University, Mainz, Germany*

(*Received 16 June 2010; final version received 23 November 2010*)

We report a novel scheme to improve the effective transmission of a standard interference filter, and demonstrate over 97% passband transmission. Such high efficiency is critical for quantum information applications, e.g. high-efficiency single-photon generation utilizing parametric down-conversion. The scheme can also be modified to function with a tilted filter, thereby allowing tuning of the passband frequency. In addition, the tilted configuration creates an infinite number of consecutive reflections from and transmissions through the filter, further improving the net filter transmission. Because spectral interference filters are a key element in optical quantum information experiments (both on the source and detection side, e.g. to exclude background photons as well as to determine the spectra of the desired photons), our scheme of enhanced interference filter transmission should lead to significant performance improvements in such experiments.

Keywords: interference filter; quantum information processing; nonlinear optics; heralding efficiency

1. Introduction

Spectral interference filters are used in many applications, and are a key element in optical quantum information experiments, both to exclude background photons as well as to determine the spectra of the desired photons. For example, one of the most widely used single-photon generation schemes utilizes parametric down-conversion (PDC) with random emission of correlated photon pairs – detecting one of the photons of a pair heralds the presence of the second one. The maximum heralding efficiency [1,2] of such a single-photon source is limited by the transmission and steepness of the interference filters used to define the photon's spectral mode. In some cases the filters are also needed to effectively disentangle the frequency correlations of the transmitted photons, critical for high-quality multi-photon interference effects [3]. Unfortunately, standard off-the-shelf filters have typical peak transmissions of 70–90%, and even lower average transmission in the passband. Here, we present a novel scheme to improve the effective transmission of a standard interference filter: by using polarization to recycle any reflected light, the transmission is improved from the single-pass transmission T to up to $2T - T^2 = 1 - R^2$. The predicted heralding efficiency is similarly improved. We have implemented such a scheme and achieved transmissions of over 97%. We also report a method to tune the transmission band while using a modified version of this technique in a tilted-filter configuration; this also creates multiple consecutive reflections from and transmissions through the filter, further improving the net filter transmission (in the limit of lossless elements).

2. Experiment and results

In our setup, we investigated a standard off-the-shelf interference filter (at 702 nm, FWHM bandwidth $\sim$5 µm), as well as a custom-designed high-transmission optical interference filter (center wavelength = 710 nm, FWHM bandwidth = 4.6 nm). Figure 1 shows our setup for filter transmission enhancement. As a tunable coherent light source, we used an external-cavity diode laser in the Littman configuration [4]. The cavity was neither thermally stabilized nor vibration-isolated; in order to improve the system stability, we coupled the laser beam (at the cavity's output) into a multimode fiber (MMF) and then back to free-space, before directing it into our system. The auxiliary beam-splitter (BS) is used for real-time calibration measurements of the spectrum of the laser. In this configuration we measured the typical FWHM bandwidth of the light to be $\sim$240 pm, which partially limited the spectral resolution of our measurements on the steep slopes of the filters. Replacing the MMF by a single-mode fiber (SMF), we observed

*Corresponding author. Email: jan.bogdanski@gmail.com

ISSN 0950–0340 print/ISSN 1362–3044 online

DOI: 10.1080/09500340.2010.543476
http://www.informaworld.com

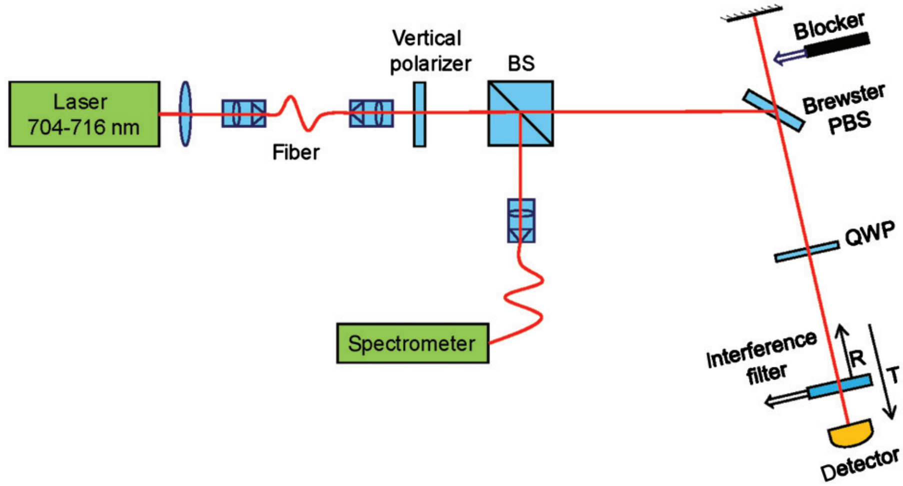

Figure 1. Transmission enhancement of an interference filter. The left side of the vertical polarizer: tunable external-cavity diode laser in the Littman configuration, coupled into a multimode fiber (MMF); BS: non-polarizing beam-splitter; QWP: quarter wave plate. The arrow attached to the filter indicates our method to measure the single-pass transmission of the filter: $T = P_{\mathrm{filter\_in}}/P_{\mathrm{filter\_out}}$. During these measurements, the 'recycling' optical path is blocked. (The color version of this figure is included in the online version of the journal.)

that the FWHM could be reduced to ~80 pm, due to the spatial filtering characteristic of the SMF. However, we also observed a 2–3% increase in intensity fluctuations – most likely due to variations in the uncoupling efficiency to the fiber – larger than we were willing to tolerate for these precision measurements.

The polarizing beam-splitter (PBS) – quarter waveplate (QWP) combination functions as an optical recycler. The vertically polarized laser beam is reflected by the Brewster PBS and the QWP converts the polarization of the beam to circular. The main part of the beam is transmitted through the interference filter and detected, e.g. by a power meter, single-photon detector, etc., depending on the application; we used a Newport power meter (No. 1830-C, precise to 1%). However, any reflected part of the beam goes back through the QWP and arrives horizontally polarized at the Brewster PBS; thus, this reflected beam is now transmitted through the PBS, bounces off the retro-reflection mirror, and is directed again to the filter, where it has a second chance to be transmitted. In this way, the bare interference filter transmission is enhanced from T to $T(1+R)=2T-T^2$, assuming there are no other losses, e.g., in the QWP, HWP, PBS, or filter itself. The measured and predicted transmission improvement for our standard off-the-shelf filter (with single-pass peak transmission of 60%) is shown in Figure 2; Figure 3 shows the results for our custom-designed filter, which already provides a high passband transmittance (around 90%)–the enhancement scheme increases it to 97%. Ideally, the theoretical improvement should be even higher (99%), assuming

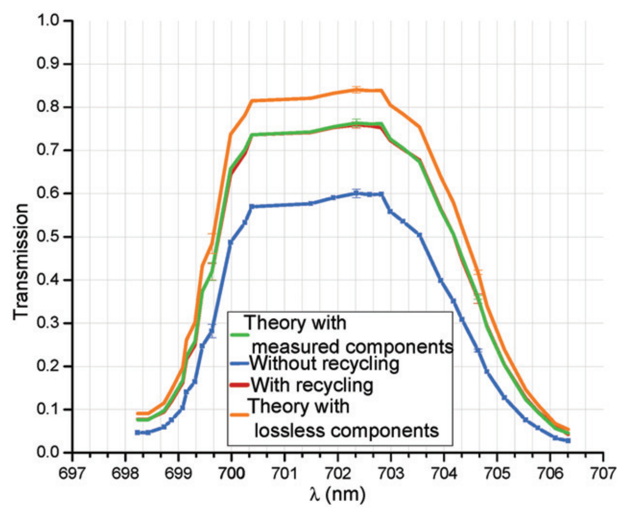

Figure 2. Standard-off-the shelf interference filter transmission, with and without recycling, and theoretical predictions, both assuming lossless components ('ideal') and using measured component values ('real'). (The color version of this figure is included in the online version of the journal.)

lossless components. However, we have found that assuming that ~3.6% of the incident light is absorbed/scattered per cycle (e.g. in the filter, PBS, etc.) explains the difference between our measurements and the ideal theory; this loss is in reasonable agreement with our directly measured values for the various components.

In addition to increasing the peak transmission of an interference filter, the recycling trick has the benefit

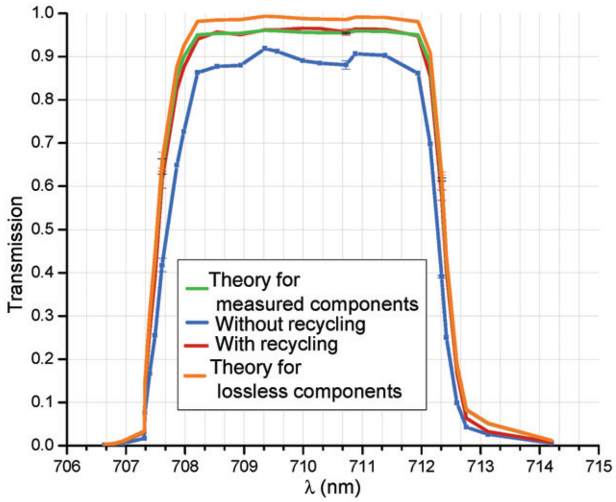

Figure 3. Custom-designed filter transmission, with and without recycling, and theoretical predictions, both assuming lossless components ('ideal') and using measured component values ('real'). (The color version of this figure is included in the online version of the journal.)

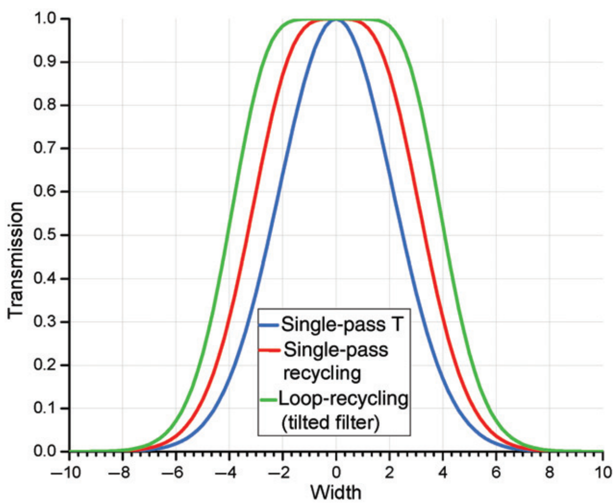

Figure 4. Theoretical comparison of the modified filter spectra, using the methods presented here. The *x*-axis is an arbitrary wavelength scale (assuming the other components in the scheme function over all the wavelengths of interest). (The color version of this figure is included in the online version of the journal.)

of improving the average transmission as well, which is critical in some applications. For example, if the filters are used as part of a parametric down-conversion source to produce single photons (heralded by the detection of one member of the pair) high efficiency is only achieved if the average transmission over the entire passband of the filter is close to unity – ideally one would want a perfect 'top-hat' filter shape. Figure 4 shows the effect of the recycling technique on an ideal Gaussian-shaped transmission spectrum (as well as the performance using the more sophisticated loop-recycling scheme discussed below). Because the edges of the transmission curve fall off more sharply, the net filter transmission after recycling more closely approximates the desired top-hat filter shape. For the case of a Gaussian-shaped filter with unit peak transmission, the resulting expected heralding efficiency in the downconversion-based single-photon source described above increases from 70.7% to 78.8% using the recycling technique (and further increases to 83.2% using the loop-recycling approach); obviously, the relative improvement would be even higher if the initial peak transmission were less than unity. For the custom-designed filter shown in Figure 3, the recycling transmission improvement corresponds to a theoretical heralding efficiency increase from 83.7% to 89.3%.

3. Tilted-filter configuration

The filter transmission enhancement scheme can be extended and improved by tilting the filter, as shown in Figure 5. In particular, we can controllably adjust the filter's central transmission wavelength (to lower values) by tilting it; there may also be a reduction in the single-pass transmission in this case, but this will be somewhat mitigated by our recycling scheme. Similar to the non-tilted single-cycle setup (Figure 1), the polarizing beam-splitter (PBS) – half waveplate (HWP) combination functions as an optical recycler: the horizontally polarized laser beam is transmitted by the PBS and the main part of the beam is transmitted through the interference filter (arriving horizontally polarized at the detector). However, a reflected part of the beam goes back through the HWP and arrives vertically polarized (after reflection by the tilted mirror) at the PBS. This first-recycled beam is then reflected by the PBS, and directed again to the filter, where it has a second chance to be transmitted (now with vertical polarization). The reflected part of the first-recycled beam goes back through the HWP and arrives horizontally polarized at the PBS. Thus, this second-recycled beam is transmitted through the PBS, bounces off the retroreflection mirror and passes back through the PBS and HWP (where its polarization is changed back to vertical); at the filter it has a third chance to be transmitted, but now it is propagating toward the QWP-mirror combination, which together reflects the beam with horizontal polarization. This beam then has an opportunity to be reflected from the back-side of the filter toward the detector, or be transmitted through the filter toward the HWP.

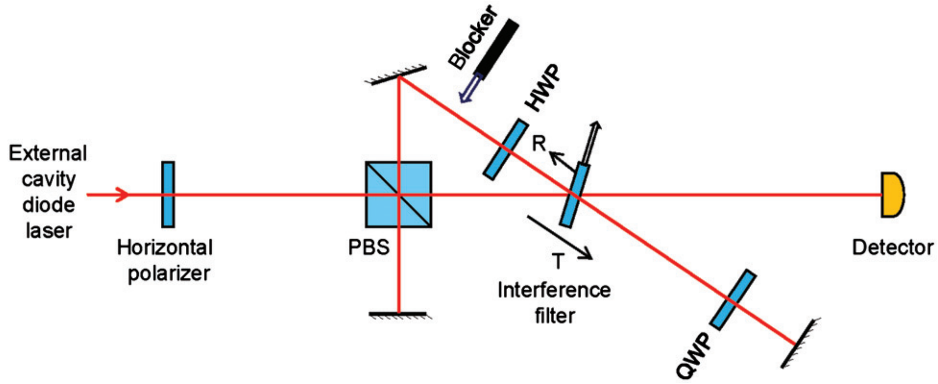

Figure 5. Transmission enhancement of a filter in the tilted configuration. The prediction for the enhanced filter transmission is given in the text. As before, the arrow by the filter indicates our method to measure its single-pass transmission, and the need to block the recycling path during these measurements. (The color version of this figure is included in the online version of the journal.)

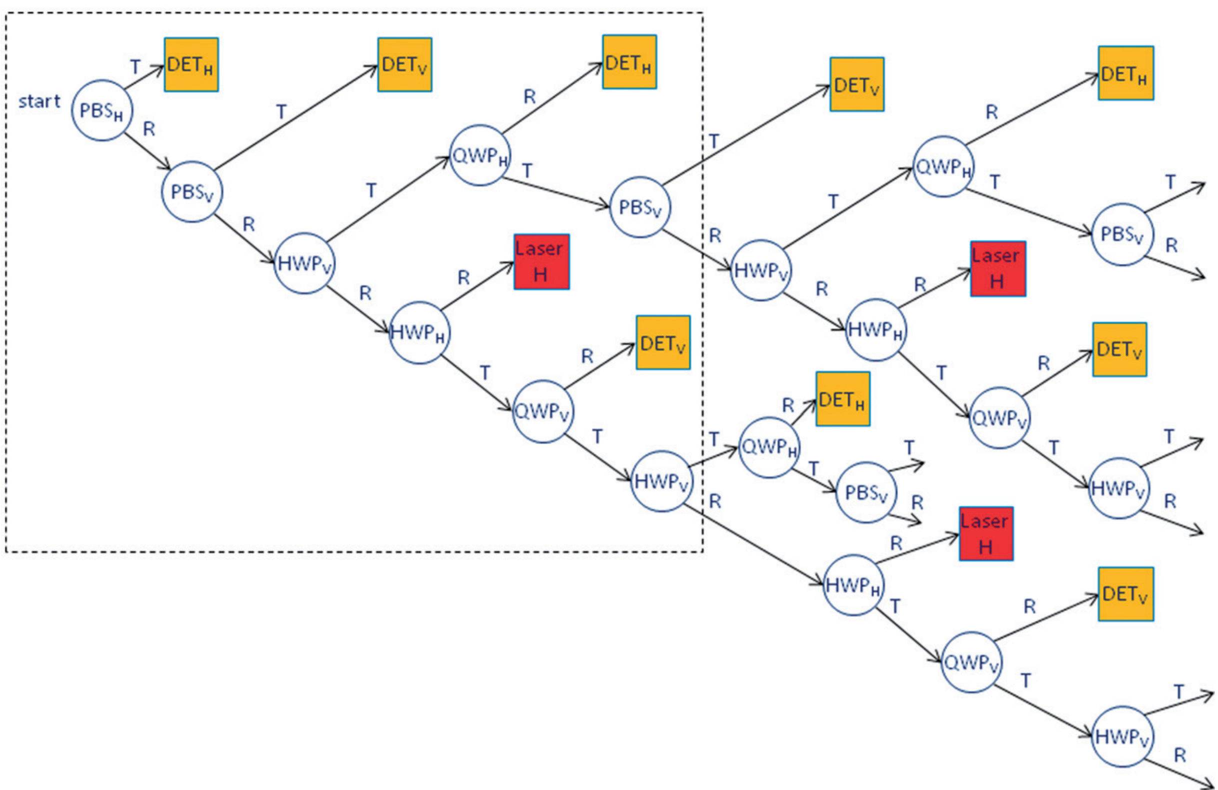

Figure 6. Transmission graph of the tilted filter. The circles show the reflection directions and polarization states of the light at the interference filter. PBS_H and PBS_V denote counterclockwise reflections (horizontal and vertical polarization, respectively) of the beam incident from PBS, HWP_H and HWP_V clockwise reflections of the beam incident from HWP, and QWP_H and QWP_V clockwise reflection of the beam incident from QWP. The orange rectangles show the polarization of the light at the detector, while the red ones show the polarization of the light reflected back to the laser source (and thus not detected). The rectangle indicates the states used in the Appendix to derive the complete set of transmission relations; the rest of the diagram indicates the repetitive cyclic nature of the setup. (The color version of this figure is included in the online version of the journal.)

In order to keep track of the somewhat complicated evolution of the beam, we found it helpful to develop the theoretical transmission diagram shown in Figure 6, where the circled polarizations describe the state of the light at the filter only (the intermediate states are not shown). From Figure 6 we can see that consecutive reflections and transmissions create repeated patterns. Using these one can calculate a

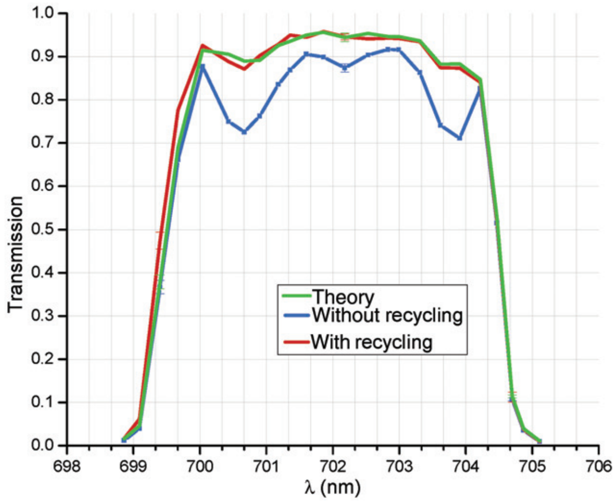

Figure 7. Tilted interference filter transmission, with and without recycling, and theoretical prediction. (The color version of this figure is included in the online version of the journal.)

closed-form solution for the net transmission T_{enhanced} (see the Appendix for its derivation) assuming lossless components and neglecting any polarization dependence of the filter transmittance T and reflectance R:

$$T_{\text{enhanced}} = 1 - \frac{R^4}{1 - 2R + 4R^2 - 2R^3}. \qquad (1)$$

The predicted and measured transmission improvements of the same custom-designed filter used in the non-tilted setup (Figure 3) are shown in Figure 7. As with the non-tilted setup, the ideal theoretical improvement should be even higher (99%), assuming lossless components, but this is again limited by the filter absorption in the passband, which in the tilted case can be a function of both polarization and wavelength.

4. Discussion

Despite their value in improving filter (or other optical element) transmission, the schemes presented here may nevertheless not be suitable for applications requiring a single-time filter response (i.e. without any echo), as is often the case for many telecommunication and other signal-processing applications. Using optimized micro-optics, one could envision a system where the total time added by the recycling optics is quite small, e.g. below 100 ps (at this level one may need to care about unwanted coherent interference effects, i.e. if the source coherence length exceeds the recycle delay). However, even such short differences in arrival times corresponding to the various recycled photon paths could serve as a limitation for some applications at the quantum level. For example, when used as a spectral filter for a single-photon source, the multiple arrival times enlarge the Hilbert space of the photon by effectively introducing time bins. As long as this happens immediately prior to detection, it is likely not a serious issue. On the other hand, if the photons are to be passed onto another optical circuit after the filter, then the uncertainty in the temporal location of the photon would likely degrade the performance of the subsequent circuit, particularly if it involves two-photon interference. Finally, another restriction of both configurations discussed above is that they require polarized inputs, which for some applications could be limiting; for many optical quantum information processing applications, however, one needs to measure the polarization anyway, so this analysis can simply be included before the present scheme.

In summary, we achieved improved transmission of an optical interference filter, in both a single- and a loop-recycling scheme, with experimental results closely matching our theoretical predictions (after accounting for various losses). In addition to improving the maximum transmission of a filter, these schemes can also be utilized to achieve improved heralding efficiency in single-photon sources. One should note, however, that even our best filter still only had a maximum projected heralding efficiency of ~89%, so more work is needed in this area.

Acknowledgements

The authors acknowledge Andrew White, Department of Physics, University of Queensland, Australia, for his original idea of improving the interference filter transmission. The authors also acknowledge support from the IARPA-funded ARO Project (W911NF-05-0397), NSF Grant No. PHY-090386, and US-Israel Binational Science Foundation (BSF No. 2008032).

References

[1] Pittman, T.B.; Jacobs, B.C.; Franson, J.D. *Opt. Commun.* **2005,** *246,* 545–550.

[2] Castelletto, S.; Degiovanni, I.P.; Schettini, V.; Migdall, A. *Metrologia* **2006,** *53,* S56–S60.

[3] U'Ren, A.B.; Banaszek, K.; Walmsley, I.A. *I. J. Quant. Inf. Comput.* **2003,** *3,* 480–502.

[4] Harvey, K.C.; Matt, C.J. *Opt. Lett.* **1991,** *16,* 910–912.

Appendix

To simplify the derivation of the net tilted filter transmission (Equation (1)), we neglect any polarization dependence of the filter transmittance T and reflectance R. For large tilt angles this dependence would need to be included. In order to do the derivation and more explicitly show the three main repeated reflection patterns of the tilted filter, the rectangle in the transmission graph of the tilted filter (Figure 6) indicates the states used to derive the complete set of transmission relations; the rest of the diagram indicates the repetitive cyclic nature of the setup. Following the graph we find:

$$T_{\mathrm{PBS_H}} = T + RT_{\mathrm{PBS_V}} \tag{2}$$

$$T_{\mathrm{PBS_V}} = T + RT_{\mathrm{HWP_V}} \tag{3}$$

$$T_{\mathrm{HWP_V}} = TT_{\mathrm{QWP_H}} + RT_{\mathrm{HWP_H}} \tag{4}$$

$$T_{\mathrm{QWP_H}} = TT_{\mathrm{PBS_V}} + R \tag{5}$$

$$T_{\mathrm{HWP_H}} = TT_{\mathrm{QWP_V}} \tag{6}$$

$$T_{\mathrm{QWP_V}} = TT_{\mathrm{HWP_V}} + R. \tag{7}$$

Solving the above equations in regards to T_{PBS_H} leads to the following final result:

$$T_{\mathrm{PBS_H}} = \frac{T - 2T^3R + RT - T^3R^2 + TR^3 + TR^4}{1 - 2T^2R}. \tag{8}$$

Assuming $T + R = 1$ (no loss case) leads to

$$T_{\mathrm{PBS_H}} = T_{\mathrm{enhanced}} = 1 - \frac{R^4}{1 - 2R + 4R^2 - 2R^3}. \tag{9}$$